Lattice dynamics study and specific heat of CsH_2PO_4 and CsD_2PO_4

Ya. Shchur
Institute for Condensed Matter Physics, vul. Svientsits'kogo 1, 79011 L'viv, Ukraine
(Received 11 January 2006; revised manuscript received 7 April 2006; published 1 August 2006)

This paper reports the results of lattice dynamics simulation of CsH_2PO_4 and CsD_2PO_4 crystals in paraelectric and ferroelectric phase using a semiempirical atomistic model based on the Coulomb, short range, covalent, and van der Waals interactions. The peculiarity of the two types of hydrogen bonds is taken into consideration too. The tunneling of protons (deuterons) on the one type of hydrogen bonds above the phase transition point was simplified through keeping the $H(D)$ atom position at the middle in hydrogen bonds. Phonon density of states, partial density of states, isotropic temperature factors, and specific heat were calculated. The computed phonon frequencies are particularly useful in interpreting the complicated Raman and IR spectra of these hydrogen-bonded crystals. The specific heat experimental data, reported by two groups of authors, contradict each other. The results of the given simulation may be helpful in establishing the real temperature behavior of specific heat.

DOI: 10.1103/PhysRevB.74.054301 PACS number(s): 63.20.Dj, 65.40.Ba, 77.80.−e

I. INTRODUCTION

The KH_2PO_4 (KDP) type crystals have a long history of their investigation. They became the classical model crystals in investigating the phenomenon of ferroelectricity and in probing the different unique research techniques. Various kinds of experimental and theoretical methods were employed in studying the physical properties of these compounds (see, e.g., textbooks[1,2]). However, one cannot claim that all the aspects of physical properties and phase transition mechanism have already been properly understood. To a greater extent it concerns the low symmetry monoclinic representatives of KDP family compounds, namely CsH_2PO_4 (CDP) and its deuterated analog CsD_2PO_4 (DCDP) crystals.

The chief experimental methods probing the underlying physical mechanisms of phase transformation are Raman scattering and IR research. However, due to the mixed nature of spectra (internal vibrations of PO_4 tetrahedra are often overlapped with hydrogen bond vibrations) and the appearance of high order Raman scattering and Fermi resonance effects in the spectra, the available spectroscopic data[3–5] turned out to be rather problematic for adequate interpretation.

The problem is aggravated by the fact that the methods of IR spectra analysis commonly used in interpreting of the IR data in higher symmetry systems (e.g., Kramers-Kronig approach) are inappropriate for proper analysis of IR spectra reflected from a monoclinic crystal plane. A special three-polarization measurement technique is needed to determine the correct parameters of phonon modes in IR spectra taken from monoclinic plane.[6–8] So far this method has not been utilized in investigating the monoclinic KDP type crystals. In the work[5] a qualitative attempt was made to perform an angle scanning of IR spectra measured in CDP and DCDP. However, the results were not fitted using the proper mathematical technique.[6–8] Therefore, all polar modes of B_u symmetry (in symmetrical phase) of CDP (DCDP) crystals can be treated as unknown.

There are rather contradictory experimental data concerning the temperature dependence of the C_P specific heat of CDP and DCDP presented by two groups of investigators.[9,10] The difference was observed not only in the temperature evolution of specific heat but even in the magnitude of C_P (the difference reaches 25% for CDP). Therefore, the main purpose of this work is to construct a semiphenomenological model of lattice dynamics of CDP and DCDP crystal suitable for interpreting the rather complicated spectroscopic and heat capacity experimental data. We used an atomistic potential taking into account Coulomb, short range Born-Mayer type, covalent, and van der Waals interactions. Peculiar character of hydrogen bonds was taken into consideration too.

II. CRYSTAL STRUCTURE

CDP (DCDP) crystal belongs to monoclinic $P2_1/m$ group[11,12] ($Z=2$) at room temperature and ambient pressure. The crystal structure is depicted in Fig. 1. PO_4 tetrahedra are connected by the short (2.48 Å) O_3-$H_2\cdots O_4$ hydrogen bonds into chains running along the twofold b axis. The chains of PO_4 groups are linked into layers by the longer (2.54 Å) O_1-$H_1\cdots O_2$ hydrogen bonds.[11] The H_2 (D_2) atoms are disor-

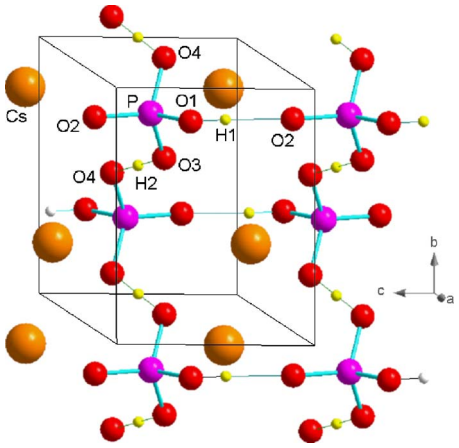

FIG. 1. (Color online) Crystal structure of CDP at room temperature.

TABLE I. Effective parameters used for simulation in paraelectric and ferroelectric phase of CDP and DCDP.

Type of ion, k	Cs	P	O_1	O_2	O_3	O_4	H_1, H_2	
$Z(k)$	0.978	1.94	−1.14	−0.91	−0.984	−0.984	0.55	Paraelectric
$R(k)$ (Å)	2.628		1.436	1.166	1.378	1.378		phase
$Z(k)$	0.978	1.94	−1.14	−0.91	−0.91	−1.058	0.55	Ferroelectric
$R(k)$ (Å)	2.628		1.436	1.166	1.166	1.436		phase

	PO_4		O-H···O		O_1-H_1···O_2		paraphase O_3-H_2···O_4	ferrophase O_3-H_2	ferrophase O_4···H_2
r_{01} (Å)	D_1 (eV)	n_1 (Å^{-1})	D_2 (eV)	n_2 (Å^{-1})	r_{03} (Å)	r_{04} (Å)	r_{02} (Å)	r_{02} (Å)	r_{05} (Å)
1.616	24.345	3.2	11.69	1.93	1.605	1.235	1.378	1.572	1.245

dered above the ferroelectric phase transition point T_C=152 K in CDP crystal (T_C=267 K in DCDP) and become ordered in one of the two possible off-center sites below the phase transition into ferroelectric phase [space group $P2_1$ (Z=2)].[13] The H_1 (D_1) atoms are ordered on the hydrogen bonds at all temperatures.

In paraelectric phase 48 normal phonon modes are classified in Brillouin zone (BZ) center as follows $\Gamma: 13A_g+8B_g+11A_u+16B_u$. All *gerade* normal modes (A_g and B_g) are Raman active and all *ungerade* modes (A_u and B_u) are active in IR spectra. In ferroelectric phase all normal modes ($24A+24B$) become visible both in Raman scattering and in IR spectra.

III. MODEL

Lattice dynamics simulation of CDP and DCDP crystals was done both in the para- and ferroelectric phase using a quasiharmonic atomistic approach.[14] The principal obstacle in performing this type of modeling in the case of CDP crystal is the presence of *a priori* anharmonic hydrogen bonds. Moreover, the existence of two kinds of hydrogen bonds, one of them being asymmetric (O_1-H_1···O_2), complicates an adequate description of lattice dynamics and forces us to increase the number of model parameters. The following form of interatomic potential[15] successfully used in simulating the number of different type compounds[16–18] was utilized:

$$\Phi(r_{kk'}) = \frac{e^2}{4\pi\varepsilon_0}\frac{Z(k)Z(k')}{r_{kk'}} + Sa\exp\left(-\frac{br_{kk'}}{R(k)+R(k')}\right) + D_{0j}\exp\left(-\frac{n}{2}\frac{(r_{kk'}-r_{0j})^2}{r_{kk'}}\right) - \frac{w}{r_{kk'}^6}, \quad (1)$$

where a=1822 eV and b=12.364.[19] The first and the second terms in this expression correspond to Coulomb and short-range interactions, respectively. $Z(k)$ and $R(k)$ are the effective charge and radius of the k atom. The third and the fourth terms describe the covalent bonding within the PO_4 groups and van der Waals interactions, respectively. The same covalentlike form of potential was utilized in simulating the oxygen-hydrogen interactions within the hydrogen bonds. Model parameters used in the simulation are listed in Table I. S and w were chosen to be 1.985 and 59 eV Å^6, respectively, for modeling oxygen-oxygen interactions within the same phosphate groups at all temperatures. Simulating the interactions between the atoms of all other types we put S and w to be equal 1 and 0, respectively. Since the $H_2(D_2)$ atoms are disordered between two off-center positions in paraelectric phase, we treated them to be located in the center of O_3-$H_2(D_2)$···O_4 bonds (in order to preserve the center symmetric $P2_1/m$ group). Therefore, the same r_{02} parameter was used for O_3-$H_2(D_2)$ and O_4-$H_2(D_2)$ interactions, whereas two different r_{03} and r_{04} parameters turned out to be indispensable for proper description of the O_2-$H_1(D_1)$ and O_1-$H_1(D_1)$ interactions within the O_1-$H_1(D_1)$···O_2 bonds ordered even in paraelectric phase. Below the phase transition point we used the slightly modified values of effective charges and radii for O_3 and O_4 ions. Instead of one r_{02} parameter in paraelectric phase we introduced two r_{02} and r_{05} parameters in ferroelectric phase. This seems quite natural due to the ordering of $H_2(D_2)$ atoms on the O_3-$H_2(D_2)$···O_4 bonds below the phase transition and the subsequent charge redistribution of O_3 and O_4 ions.

All parameters were refined after optimizing the experimental crystal structure of CDP (at[11] T=297 K and[12] T=80 K) and DCDP (at[20] T=283 K and[12] T=80 K) concerning the lattice stability conditions. The same parameters were used for lattice dynamics simulation both of CDP and DCDP crystals.

IV. RESULTS AND DISCUSSION

A. Phonons near BZ center

Calculated phonon frequencies of CDP and DCDP crystals in paraelectric phase near BZ center are presented in Table II. The predominant type of phonon modes [internal stretching or proton (deuteron)] obtained by means of the *eigen*vector analysis is indicated for high frequency modes. The low and medium frequency modes are of mixed type. There is no experimental data for LO modes of A_u. The calculation of phonon spectrum was scanned in the (a,c) plane to find the direction of dipole moment φ (counting

TABLE II. Comparison between the calculated and experimental (Ref. 3) BZ center phonon mode frequencies in cm^{-1} (1 cm^{-1}=0.124 mEv) in paraelectric phase of CDP and DCDP. The ϕ angles are expressed in degrees. All the experimental IR modes of B_u symmetry are mixed TO-LO ones. Experimental data were taken at T=300 K. The simulation was done at T=297 K for CDP and at T=283 K for DCDP. ν_1=940, ν_2=420, ν_3=1020, and ν_4=560 cm^{-1} are the internal modes of the free PO_4 tetrahedra (Ref. 21). Prime near $H_2(D_2)$ means that the corresponding proton (deuteron) frequencies were calculated assuming the $H_2(D_2)$ atoms at the middle of O_3-$H_2(D_2)\cdots O_4$ bond.

A_g		B_g		A_u			B_u			
				Cal.		IR	Cal.			
Cal.	Raman	Cal.	Raman	*TO*	*LO*	*TO*	*TO*	*LO*	ϕ	IR
					CDP					
46	42	46	46	65	76	74	64	79	−44	76
57	49	80	61	82	112	100	92	112	44	106
75	75	117	110	193	198		151	156	−83	146
124	118	234	234	218	221	220	244	256	−7	
233	219	370	428	361	375	352	283	319	−62	389
295	389	548	550	H_2' 753	795		478	493	20	509
459	471	H_1 1007		H_2' 808	810	872	H_2' 828	842	18	897
546	541	ν_3 1144	1086	H_1 956	1006	948	ν_1 897	957	41	966
ν_1 909	921			ν_3 1102	1193	1124	H_2' 978	982	20	1072
ν_3 1059	991			H_2' 2844	2847	2740	H_1 1029	1047	−35	1154
H_1 1084	1128						ν_3 1085	1149	−42	1227
ν_3 1203	1223						ν_3 1178	1244	69	1303
H_1 2302	2350						H_1 2297	2330	12	2300
							H_2' 2870	2892	−54	
					DCDP					
43	42	45	45	64	86	74	62	80	−39	76
54	49	84	61	87	109	102	90	113	44	97
70	75	110	108	176	182		154	158	−87	146
127	118	221	223	208	211	208	225	239	−17	
231	211	358	417	351	358	352	255	284	−68	
290	384	537	535	D_2' 488	529	485	469	477	−2	502
448	481	D_1 767		D_2' 544	545	627	D_2' 586	644	11	539
537	538	ν_3 1145	1096	D_1 708	779	690	D_2' 673	693	61	707
D_1 799	883			ν_3 1097	1147	1160	D_1 789	826	72	888
ν_1 930	911			D_2' 2062	2064	2000	ν_1 913	928	−41	976
ν_3 1068	1014						ν_3 1034	1078	−54	1080
ν_3 1180	1155						ν_3 1159	1191	52	1180
D_1 1680	1755						D_1 1676	1706	14	1750
							D_2' 2082	2101	−56	2100

counterclockwise from the c axis) and values of LO frequencies of B_u symmetry. Note, the B_u frequencies reported by Marchon and Novak[3] correspond to the intermediate values between TO and LO ones. It is caused by the fact that the directions of two principal axes of dielectric tensor lying in monoclinic plane may vary with frequency.[22] Consequently, the methods of the IR data analysis commonly used for higher symmetry crystals (Kramers-Kronig approach) are inapplicable to the analysis of the spectra reflected from the monoclinic (a,c) plane, since the dielectric tensor cannot be simultaneously diagonalized over the whole frequency range scanned experimentally. This physical aspect has not yet been taken into account in the previous IR investigation of CDP crystals.

As seen from Table II, there is a reasonable agreement between the simulated and experimental frequencies for the majority of normal modes. The average discrepancy for frequencies of A_g, B_g, and A_u symmetry is around 7%, 8%, and 6%, respectively, for both compounds. The disparity between the theory and experiment increases for some modes in the low and intermediate frequency region [e.g., 295 cm^{-1} (A_g, CDP) and 290 cm^{-1} (A_g, DCDP)] corresponding to the external and bending internal vibrations. This may be explained by the fact that the current simulation was performed within

TABLE III. Comparison of the calculated and experimental ultrasonic wave velocities (in m/s) of CDP and DCDP in paraelectric phase. Directions are indicated in Cartesian system $x \perp (b,c), y \| b, z \| c$.

Direction of wave propagation	Direction of wave displacement	CDP (T=297 K)		DCDP (T=283 K)	
		Expt.[a]	Calc.	Expt.[b]	Calc.
100	100	3047	2999	3152	2794
100	010	1688	1744		1712
100	001	1133	947	1163	1040
010	010	2878	2985	2940	2892
010	100	1788	1563		1605
010	001	1416	1273	1514	1400
001	001	4540	4976		5103
001	010	1586	1723		1734
001	100	1153	1360		1530

[a]Reference 23.
[b]Reference 24.

the $P2_1/m$ symmetry of paraelectric phase. However, according to the x-ray structural data of DCDP crystal in paraelectric phase the authors of the work in Ref. 20 suggested that PO_4 groups are located in two equioccupied sites around the mirror plane. This causes the violation of the selection rules of $P2_1/m$ group. This violation was really observed in Raman and IR spectra of both CDP and DCDP crystals.[3] Another source of disagreement with experiment is keeping the $H_2(D_2)$ atoms at the middle of short hydrogen bonds assumed within the current simulation. This has a certain influence not only on the frequencies of $H_2(D_2)$ vibrations but affects both the internal and the external librational modes of PO_4 groups. Hence, the calculated frequencies (Table II) correspond to the idealized center-symmetric structure of crystals under investigation. Therefore, all the "redundant" frequencies observed in Raman and IR spectra of CDP (A_g: 561, 1700, 1750, 2250, 2750 cm^{-1}, B_g: 515 cm^{-1}, A_u: 390, 476, 1016, 1244, 1740, 2660, 2300 cm^{-1}, and B_u: 544, 2660, 2300 cm^{-1}) and DCDP (A_g: 531, 949, 1345, 1420, 1710, 1980, 2090 cm^{-1}, B_g: 505 cm^{-1}, A_u: 385, 865, 917, 956, 1034, 1725 cm^{-1}, and B_u: 532 cm^{-1}) (Ref. 3) at room temperature should be treated as the result of violating the $P2_1/m$ symmetry, high order scattering, and Fermi resonance. This may explain the discrepancy between simulation and experiment especially for frequencies corresponding to the vibrations of phosphate PO_4 groups.

The comparison between the ultrasonic wave velocities estimated from the slopes of acoustic phonon branches and experimental data[23,24] in paraelectric phase is presented in Table III. As one can see from this table, there is a reasonable agreement between the simulation and experiment for most velocities. However, a large deviation of nearly 16% and 18% is observed for two lowest velocities of the semitransverse acoustic wave propagated along x and z directions and polarized along z and x axes, respectively. It may be explained by the sharp angular anisotropy of this semitransverse wave in (x,z) plane detected experimentally.[23] Therefore, even a small inaccuracy in the crystal alignment may lead to the essential change in the ultrasonic wave velocity propagated in (x,z) plane.

TABLE IV. Comparison between the experimental (Ref. 3) and calculated BZ center phonon mode frequencies of A symmetry (in cm^{-1}) in ferroelectric phase (T=80 K) of CDP and DCDP.

CDP				DCDP			
Calc.	Expt.	Calc.	Expt.	Calc.	Expt.	Calc.	Expt.
38	46	H_2 838		42	45	D_2 635	628
56	54	H_2 872	872	57	54	D_2 670	702
73	74	ν_1 911	921	74	74	D_1 794	
81	79	ν_3 1015	963	84	79	D_1 840	881
104	104	H_1 1050	993	110	110	ν_1 928	918
131	122	ν_3 1092		138	122	ν_3 1026	1011
202	205	H_1 1138	1134	197	215	ν_3 1098	1155
219	219	ν_3 1217	1219	215	217	$\nu_3$1185	1160
289		H_1 2528	2340	285		D_1 1819	1760
310	362	H_2 2703	2730	307	358	D_2 1945	1970
365	388			357	385		
471	470			461	480		
543	543			532	533		

In Table IV we list the frequencies of A type (experimental frequencies of B symmetry modes were not published) calculated in ferroelectric phase (T=80 K) for both crystals. As seen in this table, there is generally better agreement between the simulation and experiment (about 4% disagreement for both crystals) as compared to the paraelectric phase data. This may be in favor of the suggestion that the PO_4 groups are disordered around mirror plane in the high temperature phase.

The frequency shift over 100 cm^{-1} between $H_2(D_2)$ modes calculated in para- and ferroelectric phase which was not observed experimentally, may be explained by the fact that we considered the $H_2(D_2)$ atoms to be placed at the central position on the hydrogen bonds in high temperature phase. As stressed above, in reality, in high temperature phase, the protons (deuterons) are in the tunneling motion between two off-center sites along O_3-$H_2 \cdots O_4$ bonds. Therefore, the arrangement of $H_2(D_2)$ along hydrogen bonds below the phase transition is accompanied by the insignificant temperature evolution of proton (deuteron) modes in experimental spectra.

Using the group theory methods[25] one may show that the A_u irreducible representation is responsible for $P2_1/m \rightarrow P2_1$ phase transition and for spontaneous polarization appearing along the crystallographic b axis. Eigenvectors belonging to A_u contain only y components of displacements of Cs, P, O_1, O_2, and H_1 atoms, whereas all x, y, and z components of atomic displacements are relevant for O_3, O_4, and H_2. However, comparing the experimental structural data for para- and ferroelectric phase[11,12,20] one may conclude that besides the displacements of all atoms along y axis (with the exception of Cs) there are the displacements of all atoms along the x and z directions also. This means that the

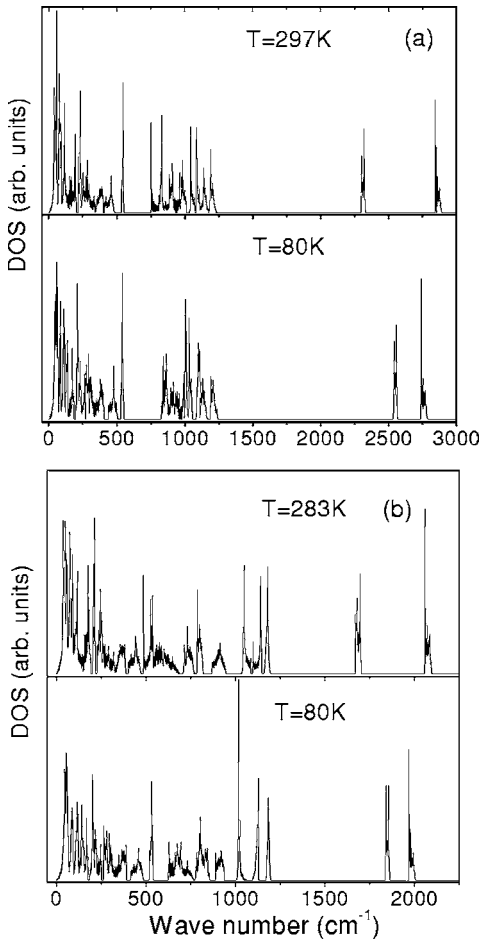

FIG. 2. Density of states calculated in paraelectric and ferroelectric phase of CDP (a) and DCDP (b).

ferroelectric phase transition is caused by multiphonon interaction. Taking into consideration that the *eigen*vectors with A_g symmetry have the x and z components for all atoms and the fact that A_u and A_g representations correlate along the $\Lambda=\mu b_2$ $(0<\mu<1/2)$ direction in the BZ, one may suggest that the interaction of A_u and A_g phonon modes evokes the ferroelectric phase transition. According to Table II, in paraelectric phase, the lowest LO mode frequency of A_u symmetry (we consider the approach to the Γ point along the Λ direction) has the value larger than three lowest A_g frequencies for both crystals. Apparently, both the softening of the lowest A_u LO phonon and multiphonon anharmonic interaction (A_u+3A_g) leads to the ferroelectric phase transition. Moreover, the real distortion of crystal structure observed at the ferroelectric phase transition in CDP and DCDP (Refs. 11, 12, and 20) does not contradict this suggestion.

B. Density of states, isotropic temperature factor, and heat capacity

Density of states was calculated within the 1/4 of irreducible BZ with rather small step (over 50 000 **k** wave vectors) using the following expression:

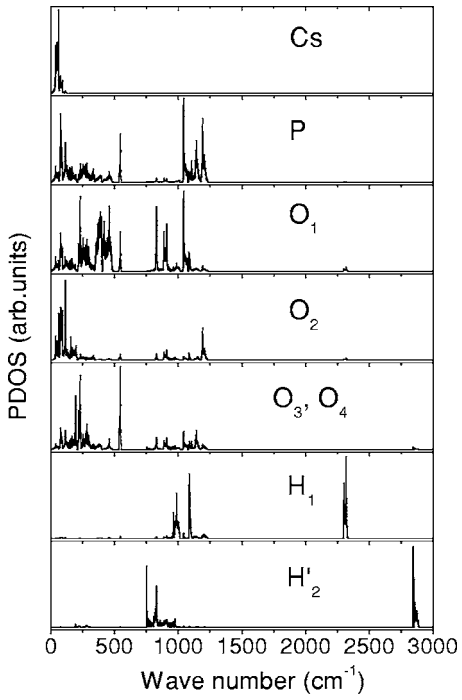

FIG. 3. Partial density of states simulated in paraelectric phase of CDP. Prime near H_2 has the same meaning as in Table II.

$$g(\omega)=A\sum_{jp}\delta(\omega-\omega_j(\mathbf{k}_p))d\mathbf{k}_p, \tag{2}$$

where A is the normalization constant, j corresponds to the phonon branch index, and p is the index of wave vector in BZ. The density of states calculated in high and low temperature phases both for CDP and DCDP crystal is shown in Fig. 2.

Partial densities of states connected with the certain kind of atoms were calculated using the relation

$$g_l(\omega)=B\sum_{\text{unit cell}}\sum_{jp}\delta(\omega-\omega_j(\mathbf{k}_p))|e_l(\mathbf{k}_p,j)|^2d\mathbf{k}_p, \tag{3}$$

where B is also normalization constant, $e_l(\mathbf{k}_p,j)$ is *eigen*vector of l-type atom in $\mathbf{k}_p$ point of BZ. Summation in [Eq. (3)] was done over all types of atoms. Partial density of states of CDP in paraelectric phase is presented in Fig. 3. As follows from this figure, heavy *Cs* atoms contribute solely in the lowest 0–90 cm^{-1} range of external lattice vibrations. The region of internal ν_2 and ν_4 bending modes of phosphate groups (350–550 cm^{-1}) is formed mainly due to the vibrations of O_1 atoms for both compounds. The range of internal ν_1 and ν_3 stretching vibrations (750–1200 cm^{-1}) is overlapped with the region of H_1 and $H_2(D_1$ and $D_2)$ normal modes. Note, there is a correlation in this range between the vibrations of O_1 and $H_1(D_1)$ atoms, which are ordered near O_1 at all temperatures. The highest frequency part [2290–2890 (CDP) and 1670–2100 cm^{-1} (DCDP)] corresponds purely to the hydrogen bond vibrations.

To check the validity of the current simulation we calculated the frequency dispersion of mean square displacements of various l atoms using the equation

TABLE V. Comparison between the calculated and experimental isotropic temperature factors B_{iso} (A^2) of CDP and DCDP. Prime near $H_2(D_2)$ means the averaged position of $H_2(D_2)$ atoms on the short hydrogen bonds in paraelectric phase.

	CDP				DCDP		
Type of ion	$T=80$ K		$T=293$ K		$T=80$ K	$T=283$ K	
	Cal.	Expt.[a]	Cal.	Expt.[b]	Cal.	Cal.	Expt.[c]
Cs	0.56	0.51	2.30	2.15	0.53	2.24	1.97
P	0.40	0.30	1.60	1.41	0.40	1.57	1.28
O_1	0.51	0.51	1.76	1.86	0.48	1.74	2.00
O_2	0.62	0.75	3.58	3.00	0.59	3.53	3.15
O_3	0.77	0.72	1.98	2.98	0.70	2.04	3.89
O_4	0.59	0.64			0.53		
$H_1(D_1)$	1.40	1.24	3.79	1.66	1.05	2.84	1.10
$H_2'(D_2')$	1.66	1.19	3.05	4.34	1.25	3.01	7.73

[a]Reference 13.
[b]Reference 11.
[c]Reference 20.

$$U_{\alpha\alpha}(l,T)=\int_0^\infty \langle U_{l\alpha}^2(\omega)\rangle_T d\omega = B\frac{\hbar}{m_l}\int_0^\infty \left(n+\frac{1}{2}\right)\frac{g_{l\alpha}(\omega)}{\omega}d\omega, \tag{4}$$

where $n=(\exp\frac{\hbar\omega}{kT}-1)^{-1}$, $g_{l\alpha}(\omega)$ is α component of partial density of state in Cartesian system. It enables us to estimate the isotropic temperature factors B_{iso} of each kind of atom $[B_{iso}=\frac{8\pi^2}{3}(U_{xx}+U_{yy}+U_{zz})]$ of CDP and DCDP crystals in both phases (Table V). As seen from these data there is a good agreement between the simulation and experimental data for all atoms in ferroelectric phase. In paraelectric phase the agreement between theory and experiment is also acceptable for heavy atoms with the exception of O_3 (O_4). The large disagreement with the experiment is observed only for hydrogen (deuteron) atoms in high temperature phase. This may be explained by the tunnel motion of the $H_2(D_2)$ atoms above phase transition whereas we treated $H_2(D_2)$ to be located at the middle of $O_3-H_2(D_2)\cdots O_4$ bonds. The $H_2(D_2)$ tunneling influences the displacement parameters of $O_3(O_4)$ atoms as well. The disparity with experiment observed for $H_1(D_1)$ atoms may be treated as the consequence of low sensibility of x-ray technique concerning the proton motion.[11,20]

The calculated densities of states were used to evaluate the lattice contribution to the C_V specific heat. Since the constant pressure C_P heat capacity is measured experimentally we made an anharmonicity correction α_V^2BVT (α_V is the volume thermal expansion coefficient, B is the bulk modulus) of the C_V, namely $C_p(T)=C_V(T)+\alpha_V^2BVT$. Experimental data were used for[26] α_V and[23] B (the same value of[23] B was utilized for both compounds). This correction plays a rather unimportant role (less than 1% at $T=300$ K) for both crystals. The computed values of C_V at certain temperature [$T=80$ K for both CDP and DCDP, and $T=297$ K (CDP), and $T=283$ K (DCDP)] were extended over the para- and ferroelectric phases, respectively, using the relation

$$C_V(T)=3N_Ak\int_0^\infty \left(\frac{\hbar\omega}{2kT}\right)^2 \csc^2\left(\frac{\hbar\omega}{2kT}\right)g(\omega)d\omega. \tag{5}$$

The results of simulation along with the experimental data are depicted in Fig. 4. There are two sets of contradictory data obtained by two groups of investigators[9,10] utilizing various techniques of experiment. As seen from Fig. 4, there is a large difference in experimental data both in the magnitude of C_P (near 25% for CDP) and in the temperature evolution of C_P for both compounds. According to[10] Imai $C_P^{CDP}(T)$ and $C_P^{DCDP}(T)$ curves cross each other near 180 K

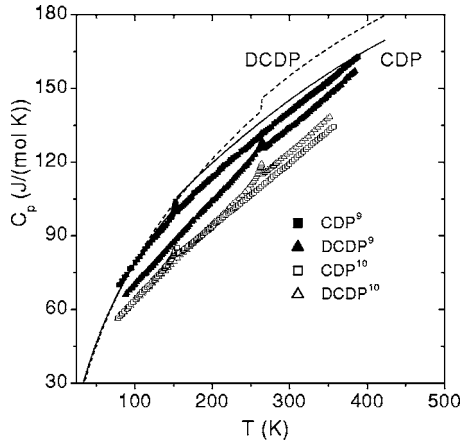

FIG. 4. The comparison between the calculated and experimental C_P specific heat data. The lines correspond to simulated values (straight line to CDP and dashed line to DCDP). Experimental data: CDP (solid squares Ref. 9, open squares Ref. 10), DCDP (solid triangles Ref. 9, open triangles Ref. 10).

and then the latter runs over the $C_P^{CDP}(T)$ at higher temperatures. Authors of the work in Ref. 9 determined the smaller values for $C_P^{DCDP}(T)$ than for $C_P^{CDP}(T)$ over the whole temperature range investigated. The temperature dependence of $C_P^{CDP}(T)$, simulated by us, corresponds within the experimental error with the data presented by Kanda *et al.*[9] However, the relation between the temperature evolutions of C_P for both crystals agrees well with the results of the work in Ref. 10. At low temperatures there is almost coincidence between the $C_P^{CDP}(T)$ and $C_P^{DCDP}(T)$ calculated curves. At $T=172$ K the both simulated curves intersect each other and for higher temperatures $C_P^{DCDP}(T)$ curve manifests larger magnitudes than $C_P^{CDP}(T)$ one.

As becomes straightforward from the relation [Eq. (5)] the lower phonon frequencies observed in Raman and IR spectra and simulated within the approach suggested in this work should result in the higher magnitude of specific heat. Therefore, the relation between the temperature evolution of C_P^{CDP} and C_P^{DCDP} reported by Imai[10] and calculated by us looks more reliable than those presented by Kanda *et al.*[9] However, the absolute values of C_P^{CDP} and C_P^{DCDP} published by Imai[10] are too low. The reasonable agreement between the experiment and optical frequencies, ultrasonic wave velocities, and isotropic temperature factors calculated in the present work enable us to suppose that the real temperature dependence of the specific heat of CDP and DCDP crystals should be close to that simulated by us. However, the additional experimental data could ultimately answer this question.

V. CONCLUSION

Semiphenomenological model of lattice dynamics of CDP and DCDP compounds involving Coulomb, short range, covalent, and hydrogen bonded interactions reliably describes the structural, spectroscopic, and acoustic data. The obtained results enabled us to interpret the intricate Raman and IR spectra of CDP and DCDP. The large number of parameters used in the model was caused by the complicated nature of various types of bonding (especially due to the presence of two kinds of hydrogen bonds) existed in the crystals under investigations. This model may be used in interpreting the spectroscopic and thermodynamic data of other hydrogen bonded crystals of KDP family.

The lattice dynamics simulation in paraelectric phase was performed within the averaged $P2_1/m$ crystal structure. Since the $H_2(D_2)$ atoms tunnel between two possible off-center positions at the short hydrogen bonds, the middle point between these sites was used as the hydrogen (deuteron) location for simulation in paraelectric phase. This had a certain influence on the calculated $H_2(D_2)$ mode frequencies and indirectly affected the internal and rotational vibrations of PO_4 groups. However, such a choice of coordinates of $H_2(D_2)$ atoms was indispensable for preserving the $P2_1/m$ symmetry within the lattice dynamics approach. Another consequence of $P2_1/m$ symmetry in paraelectric phase is the mirror symmetry of PO_4 groups. In fact, the momentum site symmetry of the PO_4 clusters deviates from the mirror symmetry, which is clearly visible in Raman and IR spectra taken at room temperature.[3,4] Therefore, the results of presented simulation enable us to indicate the normal modes "intrinsic" for macroscopic $P2_1/m$ symmetry and those arising from the violation of center-symmetric structure and other high order effects (overtones and Fermi resonance frequencies). Generally, comparing the agreement between the calculated and experimental optic mode frequencies in both temperature phases one may suggest that the model of order disorder for PO_4 phosphate groups describes more reliably the ferroelectric phase transition in this type crystal.

Results of simulation indicate the need for further experimental investigations of specific heat of CDP and DCDP crystals. New IR spectra research utilizing the three-polarization experimental technique[6–8] would also be of great interest.

ACKNOWLEDGMENT

L. Akselrud from L'viv University is gratefully acknowledged for discussions about the isotropic temperature factors of the CDP crystal.

[1] R. Blinc and B. Zeks, *Soft Modes in Ferroelectrics and Antiferroelectrics* (North-Holland, Amsterdam, 1974), p. 317.
[2] M. E. Lines and A. M. Glass, *Principles and Applications of Ferroelectrics and Related Materials* (Clarendon Press, Oxford, 1977), p. 597.
[3] B. Marchon and A. Novak, J. Chem. Phys. **78**, 2105 (1983).
[4] M. Aoki, M. Kasahara, and I. Tatsuzaki, J. Raman Spectrosc. **15**, 97 (1984).
[5] V. Videnova-Adrabinska and J. Baran, J. Mol. Struct. **156**, 1 (1987).
[6] M. V. Belousov and V. F. Pavinich, Opt. Spectrosc. **45**, 771 (1978).
[7] V. F. Pavinich and M. V. Belousov, Opt. Spectrosc. **45**, 881 (1978).
[8] A. B. Kuz'menko, E. A. Tishchenko, and V. G. Orlov, J. Phys.: Condens. Matter **8**, 6199 (1996).
[9] E. Kanda, M. Yoshizawa, T. Yamakami, and T. Fujimura, J. Phys. C **15**, 6823 (1982).
[10] K. Imai, J. Phys. Soc. Jpn. **52**, 3960 (1983).
[11] H. Matsunaga, K. Itoh, and E. Nakamura, J. Phys. Soc. Jpn. **48**, 2011 (1980).
[12] Y. Iwata, K. Deguchi, S. Mitani, I. Shibuya, Y. Onodera, and E. Nakamura, J. Phys. Soc. Jpn. **63**, 4044 (1994).
[13] Y. Iwata, N. Koyano, and I. Shibuya, J. Phys. Soc. Jpn. **49**, 304 (1980).
[14] A. A. Maradudin, E. W. Montrol, and G. H. Weiss, *Theory of Lattice Dynamics in the Harmonic Approximation* (Academic Press, New York, 1963), p. 515.

[15] S. L. Chaplot, K. R. Rao, and A. P. Roy, Phys. Rev. B **29**, 4747 (1984).
[16] S. L. Chaplot, Phys. Rev. B **45**, 4885 (1992).
[17] R. Mittal, S. L. Chaplot, and N. Choudhury, Phys. Rev. B **64**, 094302 (2001).
[18] Ya. I. Shchur, Phys. Status Solidi B **215**, 963 (1999).
[19] A. I. Kitaigorodskii and K. V. Mirskaya, Kristallografiya **9**, 174 (1964).
[20] K. Itoh, T. Hagiwara, and E. Nakamura, J. Phys. Soc. Jpn. **52**, 2626 (1983).
[21] K. Nakamoto, *Infrared and Raman Spectra of Inorganic and Coordination Compounds* (John Wiley & Sons, New York, 1997), p. 387.
[22] M. Born and E. Wolf, *Principles of Optics* (Cambridge, University Press, 1999), p. 890.
[23] S. Prawer, T. F. Smith, and T. R. Finlayson, Aust. J. Phys. **38**, 63 (1985).
[24] A. V. Kityk, Ya. I. Shchur, L. P. Lutsiv-Shumskii, and O. G. Vlokh, J. Phys.: Condens. Matter **6**, 699 (1994).
[25] G. J. Ljubarski, *Anwendungen der Gruppentheorie in der Physik* (VEB Deutscher Verlag der Wissenschaften, Berlin, 1962), p. 339.
[26] O. G. Vlokh, Ya. I. Shchur, I. S. Girnyk, and I. M. Klymiv, Fiz. Tverd. Tela (Leningrad) **36**, 2890 (1994).